

Comparative Evaluation of MVAC-LVDC SST and Hybrid Transformer Concepts for Future Datacenters

Jonas Huber^{1*}, Peter Wallmeier², Ralf Pieper², Frank Schafmeister³, and Johann W. Kolar¹

¹ Power Electronic Systems Laboratory, ETH Zürich, Switzerland

² Delta Energy Systems GmbH, Soest, Germany

³ Power Electronics and Electrical Drives (LEA), University of Paderborn, Germany

*E-mail: huber@lem.ee.ethz.ch

Abstract—A transition from state-of-the-art 400 V AC to 690 V AC or 800 V DC (± 400 V DC) distribution improves the overall power conversion efficiency of datacenter power supply systems. The latter requires megawatt-level isolated medium-voltage (MV) AC to low-voltage (LV) DC conversion stages that operate with an efficiency of at least 98%. Whereas today’s most advanced industrial MVAC-LVDC solid-state transformer (SST) prototypes do achieve this, they are highly complex and do not show any clear advantages in terms of efficiency and power density over alternative approaches that retain the low-frequency transformer (LFT) to provide isolation and decoupling from harsh MV grid realities. We thus comparatively evaluate MVAC-LVDC SSTs against such alternative concepts, i.e., LFTs with LV-side SiC PFC rectifiers, or 12-pulse rectifier systems hybridized with active filters that just provide sufficient power processing capability to achieve unity power factor operation.

I. INTRODUCTION

With more than 200 TWh/a, datacenters account for roughly 1% of the world’s total electricity consumption [1], [2]. Some forecasts [3] expect an increase beyond 2% by 2030, driven, e.g., by the growth of industrial IoT applications, which may outpace efficiency improvements. Energy bills can dominate the overall life-cycle costs of a datacenter [4]. Therefore, society and operators have an interest in maximizing the overall power usage efficiency (PUE, loosely defined as the ratio between power entering the datacenter and power being actually used by the IT equipment), which means optimizing various aspects such as cooling/HVAC systems, the efficiency of the IT equipment itself (e.g., computations per watt), and the power supply system (see Fig. 1). Increasing the efficiency of the rack-level power supply units (PSUs) is advantageous also because of the power cascading effect (upstream conversion stages must process also the losses of downstream stages). However, since the PSU efficiencies are at highest levels today, the overall power distribution system structure and especially the medium-voltage (MV) to low-voltage (LV) conversion at the grid interface must be carefully considered, too [4].

A. AC Distribution (400 V and 690 V)

As a baseline, Fig. 1a shows a state-of-the-art 400 V AC power distribution architecture, with a central low-frequency transformer (LFT) and distributed PFC rectifiers in the racks. Dry-type (i.e., oil-free) high-efficiency low-frequency transformers (LFTs) with full-load efficiencies of $\eta_{LFT} \approx 99.2\%$ exist

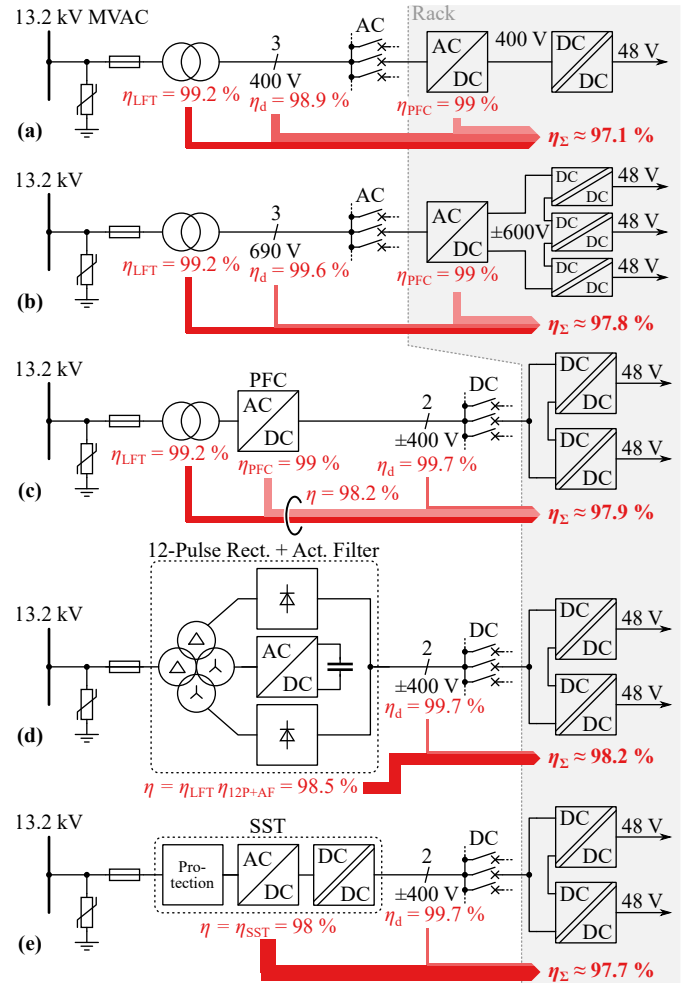


Fig. 1. Datacenter power distribution system structures and typical efficiencies η_{Σ} from MVAC to the input of the rack-level 400 V/48 V DC-DC conversion. The distribution efficiencies η_d are for transferring 1 MW over a distance of 100 m using 2000 A Delta EcoTech BL busbars, see Fig. 2. (a) State-of-the-art 400 V AC distribution. (b) 690 V AC distribution. (c) 800 V DC (± 400 V DC) distribution with MVAC-LVDC conversion employing a LFT and a centralized SiC PFC rectifier, or (d) a 12-pulse rectifier and an active filter (AF) for power factor correction, or (e) a solid-state transformer (SST).

since at least a decade [5]. New regulations¹ require similarly high efficiency for all new LFTs. Leveraging wide-bandgap

¹The European Union’s Ecodesign directive 2009/125/EC, specifically the Commission Regulation No. 548/2014, requires, e.g., $\eta_{LFT} > 99.17\%$ for 1 MVA LFTs; similar regulation exists in the U.S. (DOE 10 CF 431.196).

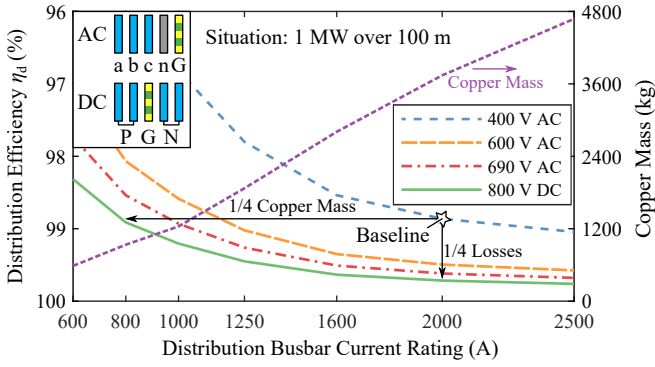


Fig. 2. Distribution efficiency η_d and copper usage for Delta EcoTech BL [8] busbars of different current ratings when transferring 1 MW over a distance of 100 m at different voltages, assuming a conductor temperature of 60 °C. The inset shows the different configurations of the conductors used for AC or DC.

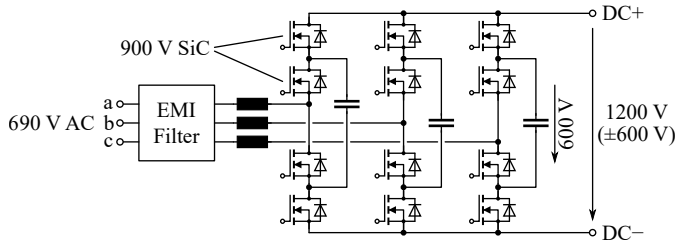


Fig. 3. Realization of a PFC rectifier for a 690 V AC grid with a three-level flying-capacitor topology using 900 V SiC MOSFETs.

(WBG) power semiconductors, PFC rectifiers with $\eta_{\text{PFC}} \approx 99\%$ are clearly feasible; in fact, significantly higher values have been demonstrated by research systems [6]. Considering a typical average distance of 100 m between the LFT and the server racks and a standard busbar arrangement (see Fig. 2), the baseline architecture achieves a full-load efficiency of $\eta_{\Sigma} \approx 97.1\%$ from MVAC input to the rack-level 400 V/48 V DC-DC PSUs.

As losses in identical distribution busbars reduce with the square of the distribution voltage (see Fig. 2), a step from 400 V AC to 690 V AC (see Fig. 1b) improves η_{Σ} . PFC rectifiers suitable for this increased AC voltage can be realized with three-level topologies (see, e.g., Fig. 3) and thus again $\eta_{\text{PFC}} \approx 99\%$. A 690 V AC architecture would thus result in a clearly improved $\eta_{\Sigma} \approx 97.8\%$ (and correspondingly lower OPEX) because of the reduced distribution losses.² Note that two or three off-the-shelf rack-level 400 V/48 V DC-DC PSUs can be stacked to handle the PFC rectifier's higher DC output voltage without affecting their conversion losses; this is why we do not include these DC-DC PSUs in the discussion and in η_{Σ} . The same applies to the uninterruptible power supply (UPS) systems, as we assume a distributed UPS with local battery storage on the 48 V level [7].

Even though a further increase of the (AC) distribution voltage level to MV has been considered in combination with rack-level MVAC-LVDC conversion (i.e., low-power MVAC-LVDC solid-state transformers, SSTs) [9]–[14], the associated overhead regarding MV-side protection equipment

² It would also be possible to reduce the distribution busbars' copper cross section (and hence CAPEX) instead, thereby accepting lower η_d and η_{Σ} , i.e., higher OPEX. A life-cycle cost (LCC) analysis would reveal the optimum balance but is beyond the scope of this paper, where we consider identical busbars and hence identical realization effort for the distribution system.

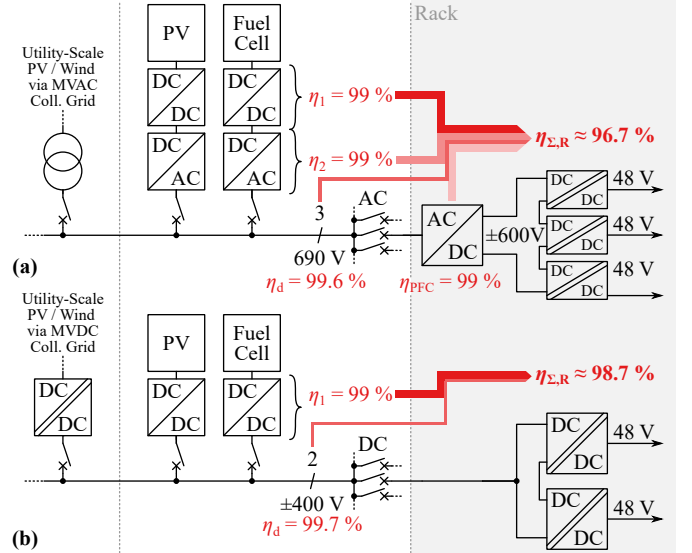


Fig. 4. Integration of roof-top photovoltaics (PV) and fuel cells (FCs) in the datacenter power supply with (a) 690 V AC or (b) 800 V DC distribution. Larger (utility-scale) renewable power infeed would occur via MVAC or MVDC [15] collector grids, and is beyond the scope of this paper.

and switchgear (disconnectors, grounding switches) seems too costly.

B. DC Distribution (800 V DC / ±400 V DC)

Alternatively, DC distribution systems are considered as well [4]. Moving, for example, to 800 V DC (advantageously symmetric ±400 V DC with respect to ground) would be possible using the same busbars with a different conductor assignment and result in slightly lower distribution losses as observed for 690 V AC (see Fig. 2). Again, two rack-level 400 V/48 V DC-DC PSUs could be stacked to interface the ±400 V DC distribution system. A DC distribution architecture comes with challenges regarding protection (DC breakers, reverse polarity and inrush current protection of the rack-level PSUs, etc.), which are, however, not in the scope of this analysis.

Regarding the integration of renewable energy sources such as rooftop photovoltaics (PV) or fuel cells (FCs) to replace diesel gensets providing backup power, an 800 V DC distribution is highly advantageous compared to a 690 V AC distribution, because a DC-AC and an AC-DC conversion stage can be omitted (see Fig. 4).

Considering the typical case of power supply from the grid, however, a central MVAC-LVDC interface is required. This paper focuses on the three conceptually different options for the realization of a MVAC-LVDC converter stage: the LFT could be retained and the PFC rectifiers centralized (see Fig. 1c and Section II). Alternatively, robust 12-pulse rectifier systems complemented by active filters (AFs) to achieve power factor correction, thus forming *hybrid transformers*, could be employed (see Fig. 1d and Section III). Finally, SSTs with medium-frequency transformers (MFTs) could be employed (see Fig. 1e and Section IV). We introduce the key characteristics of these three realization options, whenever possible taking into account published data of industrial (prototype) systems, which facilitates a comparative evaluation

(see **Section V**) regarding efficiency, power density, and further aspects such as costs and resource usage. The relevance of this analysis extends beyond datacenters [9]–[14] to other applications of MVAC-LVDC conversion such as ultra-fast EV charging [16]–[21] and high-power electrolysis [22], [23]. Note that in these applications, however, wider output voltage ranges must be covered, which typically requires additional non-isolated DC-DC conversion stages.

II. MVAC-LVDC WITH LFT AND CENTRAL SiC PFC RECTIFIER

An 800 V DC distribution can be realized by centralizing the PFC rectifier functionality and concentrating it in a single high-power unit connected to the (existing) LFT as shown in **Fig. 1c**. As it can be assumed that doing so neither changes $\eta_{\text{LFT}} \approx 99.2\%$ nor $\eta_{\text{PFC}} \approx 99\%$, the MVAC-LVDC conversion efficiency becomes $\eta \approx 98.2\%$. Considering empirical power densities of LFTs (0.3 kVA/dm³, [24]) and state-of-the-art high-power PFC rectifiers (1.4 kVA/dm³, e.g., [25]), we find a power density of $\rho \approx 0.25$ kW/dm³; actual realizations may result in somewhat lower values (switchgear, etc.).

Simply centralizing the PFC rectification functionality thus results only in a very minor improvement of $\eta_{\Sigma} \approx 97.9\%$ compared to a 690 V AC distribution as a consequence of the only slightly lower distribution losses (higher distribution efficiency η_{d}), see **Fig. 2**. On the other hand, the LFT renders this approach robust, compatible with existing MV-side infrastructure, and fully scalable to arbitrary MV levels. The realization of the high-power SiC PFC rectifier can follow proven LV converter design and construction paradigms, whereby parallel-interleaving approaches should be considered to achieve a certain degree of modularization and possibly redundancy. Furthermore, such highly efficient SiC LV AC-DC converters could advantageously also find widespread application as PV inverter stages, e.g., coupled to the MV grid via a high-efficiency LFT.

III. MVAC-LVDC HYBRID TRANSFORMERS

The MVAC-LVDC interface discussed in the previous **Section II** processes the full power with an active power electronic stage (the same applies to SSTs discussed in the next **Section IV**). This might not be necessary if a certain reduction of functionality can be accepted (e.g., datacenters do not need bidirectional power flow capability³). Entirely passive and hence highly robust 12-pulse⁴ diode rectifiers (see **Fig. 1d** and **Fig. 5a**) achieve a relatively high power factor (i.e., PFC functionality) simply by means of feeding two six-pulse diode rectifiers from two LV-side voltage systems that are 30° phase shifted with respect to each other. This can be achieved by configuring a three-winding LFT with one LV-side winding

³Datacenters are unlikely to feed power back to the grid (e.g., from UPS systems or rooftop PV); even if future datacenters would be obliged to show a grid-supporting behavior, a reduction of the consumption from the grid could be achieved by supplying the IT load (partly) with local batteries, gensets, fuel cells, or renewables, but without effectively feeding power back into the grid.

⁴18-pulse or 24-pulse designs would further improve the grid current quality, and could be interesting options for higher power levels that would anyway require paralleling of diode modules in systems with lower pulse numbers.

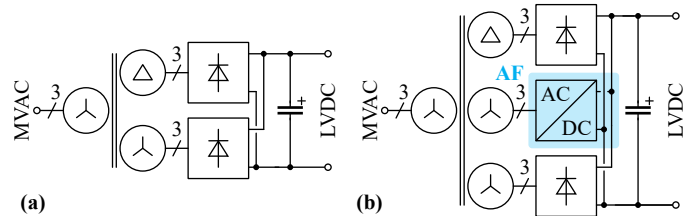


Fig. 5. (a) Completely passive 12-pulse rectifier with DC-side parallel connection. (b) 12-pulse rectifier with active filter (AF) to achieve sinusoidal grid currents and reactive power compensation, thus forming a hybrid MVAC-LVDC transformer. The optional connection to the LVDC output bus [30] enables limited reverse power flow capability (see simulation results in **Fig. 6**).

in star and the other in delta connection, see **Fig. 5a**.⁵ The superposition of the thus phase-shifted diode rectifier input currents cancels low-frequency harmonics in the MV-side grid current, most prominently the 5th and the 7th, leading to a relatively low total harmonic distortion (THD).

A. Active Filtering and Reactive Power Compensation

As proposed for *hybrid distribution transformers* [31], [32], this basic passive system can now be complemented by just the active power electronic power processing capability needed to provide certain additional functionality, e.g., sinusoidal shaping of the grid currents and compensation of the reactive power that the diode rectifiers consume. As a corresponding active filter (AF) [33], [34] processes only a fraction of the total power, the impact on the overall efficiency is reduced accordingly (*partial power processing* [35]). The AF can be connected to the MV grid via a dedicated LFT, or, advantageously, via a third LV-side winding of the main LFT as shown in **Fig. 5b**.⁶

Furthermore, if the AF is connected to the main LVDC bus (which is not necessary for the active filtering functionality as no active power is processed) as suggested in [30] and shown in **Fig. 5b**, the AF can be utilized to achieve limited (by the AF's power rating, e.g., about 25% in the case discussed here) reverse power flow. **Fig. 6** shows exemplary simulation results that demonstrate this capability.

The AF's power rating depends on the rectifier's reactive power consumption. LFTs typically feature a minimum (required by standards) short-circuit reactance of $x_k = 4\%$. This reactance defines the di/dt of the rectifier diodes' commutation and ultimately causes a fundamental-frequency reactive power consumption, $Q_1/P_{\text{dc}} \approx 20\%$. In addition, the still non-perfect sinusoidal current shape leads to a distortion reactive power consumption of $D/P_{\text{dc}} \approx 15\%$. The total reactive power consumption of a passive 12-pulse rectifier thus becomes $Q/P_{\text{dc}} = \sqrt{Q_1^2 + D^2}/P_{\text{dc}} \approx 25\%$. The derivations are beyond

⁵Even though often a DC-side interphase transformer is employed to ensure equal current sharing among the parallel-connected diode rectifiers [26], it is not strictly needed and can be omitted to reduce losses and size [27]–[29]. The LFT design must then provide sufficient leakage inductance ($\approx 4\%$) also between the two secondary windings (not only between the primary and each secondary), preventing interbridge currents and harmonic flux components in the core [27].

⁶Note that alternatively the typical DC-side interphase transformers of 12-pulse rectifiers could be replaced with *electronic smoothing inductors* (ESIs) [36]. Advanced control of these as discussed in [37] can realize sinusoidal grid currents, i.e., the approach essentially shifts the active filtering functionality from the AC side to the DC side.

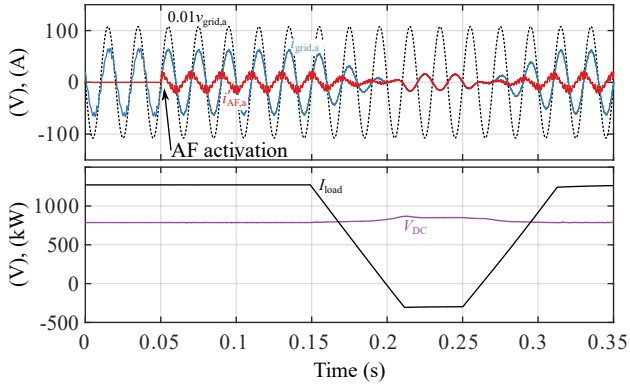


Fig. 6. Simulation of the system shown in **Fig. 5b**, i.e., a 1 MW 12-pulse rectifier with DC-bus-connected AF, demonstrating sinusoidal MV grid currents and unity power factor operation upon activation of the AF after 50 ms, as well as (limited) reverse power flow capability. The MV grid voltage is 13.2 kV, and the nominal DC output voltage is 800 V (at 50% of the nominal load). v_{grid} and i_{grid} are the MV-side grid phase-to-neutral voltage and grid current, respectively, and i'_{AF} is the AF current referred to the MV side.

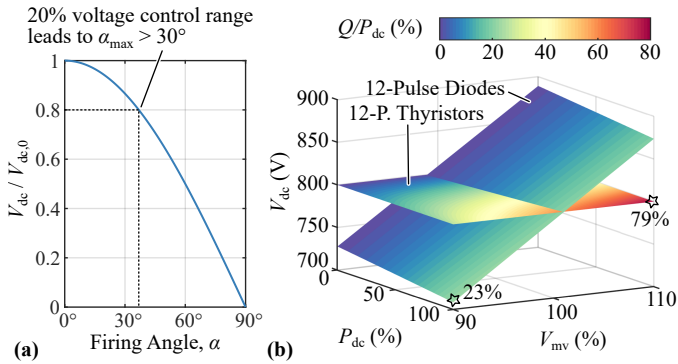


Fig. 7. (a) Idealized dependence of the output voltage of a controlled thyristor rectifier on the firing angle α ; due to the cosine-shaped control characteristic, a relatively small output voltage control range results in large firing angles and hence high reactive power consumption. (b) Output DC voltage of uncontrolled and controlled 12-pulse rectifiers in dependence of the output power P_{dc} and the grid voltage V_{mv} . The color scale indicates the total reactive power consumption, Q/P_{dc} , and the worst-case operating points are highlighted.

the scope of this paper and can be found in textbooks such as [26], or the quantities can be obtained from circuit simulations (as done here for the considered variant without a DC-side interphase transformer, resulting in a worst-case $Q/P_{\text{dc}} \approx 27.5\%$).

Considering this AF rating, assuming $\eta_{\text{AF}} = \eta_{\text{PFC}} \approx 99\%$, $\eta_{\text{LFT}} = 99.2\%$ (for the main LFT and for an assumed dedicated AF LFT), and estimating the rectifier diode losses as 0.25% based on datasheet information (Infineon DD350) and simulated device current stresses, we find a high MVAC-LVDC conversion efficiency of $\eta \approx 98.5\%$ and thus $\eta_{\Sigma} \approx 98.2\%$. Considering again $\rho_{\text{LFT}} \approx 0.3 \text{ kW/dm}^3$ and $\rho_{\text{AF}} \approx 1.4 \text{ kW/dm}^3$ based on empirical data (see above), estimating the diode rectifier's heat sink volume with a conservative cooling-system performance index (CSPI) [38] of $10 \text{ W/(Kdm}^3)$ and the volume of the 10 mF DC-link capacitor with an empirical energy density of foil capacitors (160 J/dm^3), the overall power density becomes $\rho \approx 0.22 \text{ kW/dm}^3$, which is dominated by the volumes of the LFTs. Note that the (inductive) fundamental-frequency reactive power could also be compensated using capacitor banks [39],

which would increase η at the expense of ρ and flexibility.

Note further that this hybrid approach does not strictly require the AF for a basic system operation, i.e., in case of failure, the AF could be disconnected or bypassed and the system could revert to robust 12-pulse operation while shared fall-back AFs connected to the datacenter's common MVAC bus could ensure an overall grid-friendly behavior.

B. Output DC Voltage Regulation

The output voltage of a 12-pulse diode rectifier directly reflects any deviation of the grid voltage from its nominal value (typ. $\pm 10\%$ according to EN 50160) and also reduces slightly with increasing load current (i.e., with increasing output power), see **Fig. 7b**.⁷ Output voltage control could be achieved by means of an on-load tap-changing LFT [22] without significant impact on efficiency, but with drawbacks regarding wear and tear and only limited control dynamics. Alternatively, thyristor rectifiers could control the output voltage as $V_{\text{dc}} = V_{\text{dc},\alpha=0} \cos \alpha$, where α is the firing delay angle (see **Fig. 7a**) [26]. However, first, the output voltage can only be reduced compared to that of a diode rectifier, i.e., the LFT's turns ratio must be selected such that the desired DC output voltage can be achieved at the minimum expected grid voltage. Second, as a nonzero firing angle directly translates into a corresponding additional phase-shift of the grid current, this solution would imply significant reactive power consumption of up to $Q/P_{\text{dc}} \approx 80\%$, see **Fig. 7b**, and thus a prohibitively high AF power rating.

Alternatively, a partial-power processing concept could be used to inject a compensating series voltage on the DC side (e.g., similar to [36]). However, additional MV isolation transformers would be needed and the system complexity would increase, thereby voiding the advantageous simplicity and robustness of the hybrid MVAC-LVDC transformer approach. The non-constant output DC voltage thus remains its main drawback, as then the rack-level 400 V/48 V DC-DC PSUs need to be designed for a corresponding input voltage range.

IV. MVAC-LVDC SOLID-STATE TRANSFORMERS

Solid-state transformers (SSTs) have been considered for the realization of fully controllable MVAC-LVDC interfaces for diverse applications, especially when space or weight constraints apply [40], e.g., in traction applications [41].

A. Fully Modular SSTs

Many SST concepts follow a fully modular approach by arranging a number of converter cells in an input-series-output-parallel (ISOP) configuration to handle the high MV-side voltages (series connection) and the high LV-side currents (parallel connection). Each converter cell then contains a PFC rectifier stage and an isolated DC-DC converter.

A full industrial demonstrator of a 400 kW MVAC-LVDC SST for ultra-fast EV charging applications has been presented recently [18]–[20]. This system is an impressive technical achievement and, to the knowledge of the authors, the most advanced industrial MVAC-LVDC SST prototype publicly

⁷Note that for the sake of simplicity, these results have been calculated using analytical expressions assuming the presence of a DC-side interphase transformer. The absence of the interphase transformer does not significantly change the outcome of the analysis, as simulations confirm.

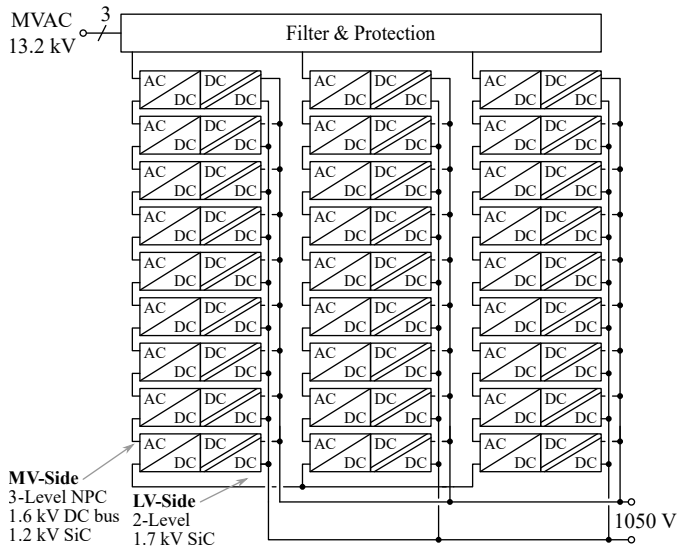


Fig. 8. Structure of the 400kW SST described in [18]–[20] with 9 cells per phase stack and hence a total of 438 individual switches and gate drive units. Each of the 27 cells processes 15kW with a PFC rectifier and an isolated DC-DC conversion stage.

documented so far. Even though requirements of ultra-fast EV charging applications may differ to some extent from those of datacenters, the system can be considered to represent the current state-of-the-art of industrial MVAC-LVDC SST systems. The SST connects to the 13.2kV MVAC grid by means of 9 cascaded converter cells per phase (27 in total) as shown in **Fig. 8**, which employ 1200 V SiC devices. Note the resulting high complexity of the multi-cell structure with a total of 438 individual switches and gate drive units (GDUs).⁸ A certain simplification could be achieved with topologies that are limited to unidirectional power flow such as proposed in [42]. The SST demonstrator achieves an MVAC-LVDC full-load efficiency of $\eta \approx 98\%$ and hence $\eta_{\Sigma} \approx 97.7\%$ results. Whereas a very high switching frequency (above 100 kHz) facilitates a high power density of the cells' high-frequency transformers ($8.5 \text{ kW}/\text{dm}^3$), it reduces to $0.44 \text{ kW}/\text{dm}^3$ for a complete converter cell (including power electronics, isolation case and housing). Finally, the power density of the overall SST system (i.e., including cabinets, input filters, and protection systems⁹) is only $\rho = 0.047 \text{ kW}/\text{dm}^3$, and the system weighs 3000 kg.

B. SSTs with Single Multi-Winding MFT

Fully modular concepts must provide the full isolation distances in each converter cell and in particular in each low-power MFT, which partly explains the power density discrepancy between MFT and system discussed above. Alternative concepts with a single multi-winding MFT have thus been proposed early on, e.g., for traction applications in [44], and later also for three-phase applications [45], [46]. Whereas ultimately more

⁸Note that the *number* of individual switches depends on the ratio between MV level and the switches' blocking voltage rating; it is unrelated to the power level.

⁹Protection of MV-connected power electronics is challenging and typically requires relatively large chokes at the AC input [43].

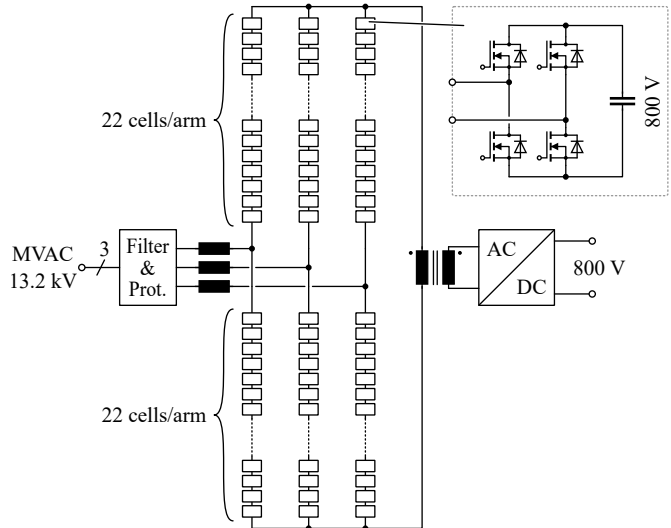


Fig. 9. MMC-based SST topology according to [52] with a single, fully rated MFT but 528 individual switches (on the MV side); in order to facilitate a comparison with **Fig. 8**, 1200 V SiC MOSFETs are considered.

compact systems may result¹⁰ (e.g., $\rho = 0.5 \text{ kW}/\text{dm}^3$ has been reported for a 3 MW MVAC-LVDC system in [49], but without information on efficiency, etc.), so far no full-scale industrial demonstrator has been publicly documented in detail.

C. MMC-Based SSTs with Single MFT

A further reduction of the isolation overhead can be expected from SST topologies that limit the modularization to the power electronics and employ only a single, fully rated MFT, i.e., that feature only a single main isolation barrier. This can be achieved by a modular multilevel (MMC) topology, which essentially uses cascaded-cells structures [50] to realize switches of higher voltage rating [51]. With a suitable control method proposed in the early 2000s, the converter cells do not need an external, isolated power supply and the MMC acts as a direct AC-AC converter between a three-phase low-frequency grid and a single-phase high-frequency transformer [52]. Whereas the single MFT is clearly advantageous, note that the complexity remains high: Considering again the same 1200 V SiC devices (operated at 800 V) as in **Fig. 8** and assuming an MV-side MFT transformer voltage that is equal to a grid phase voltage¹¹, the MMC requires 22 cells per arm and thus a total of 528 individual switches (not counting the LV-side rectifier). The approach has recently been proposed for MVAC-LVDC frontends for high-power EV charging [53], but there are no prototypes as of today.

D. SSTs with Future High-Voltage SiC Devices

Academia has explored the benefits of employing novel high-voltage SiC devices, which facilitate designs with fewer cascaded cells or without cascading at all. For example, NC State University has designed a 350kW (unidirectional) EV charger for direct connection to the 12.47kV MVAC grid [21]. Calculation results indicate $\eta \approx 98.1\%$ and $\rho \approx 1.6 \text{ kW}/\text{dm}^3$.

¹⁰For example, the shared MFT (or only its windings, see [47], [48, p. 74]) could be embedded in an oil-filled tank for isolation and cooling.

¹¹The MV-side MFT voltage is a degree of freedom to adjust the required total arm voltage vs. the current stress [52].

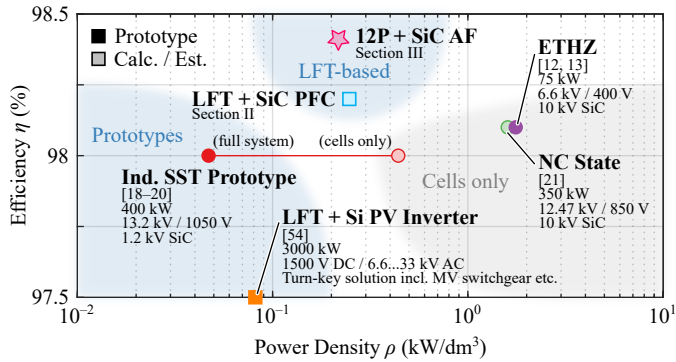


Fig. 10. Performance (efficiency at rated power, power density) comparison of SST-based and alternative MVAC-LVDC conversion solutions. Note: single-phase systems are scaled to three phases (star connection of three units).

ETH Zürich has built a 25 kW demonstrator using 10 kV SiC MOSFETs to interface a single-phase 3.8 kV MVAC grid [12], [13]. Employing soft-switching techniques for both, the AC-DC and the isolated DC-DC stage, $\eta \approx 98.1\%$ and $\rho \approx 1.8 \text{ kW/dm}^3$ have been measured experimentally. Whereas these efficiencies can be considered representative, the power densities of industrialized prototypes will be lower (cabinets, isolation coordination to standards, etc.). Configuring two of these modules in series on the AC side would facilitate the connection to a phase of the 13.2 kV grid, and arranging three such two-cell stacks in a star configuration would yield a 150 kW three-phase system requiring a total of 60 individual switches. The overall efficiency can be assumed to remain largely unaffected. Thus, high-voltage SiC devices enable a reduction of the number of modules needed to interface a given grid voltage level, and hence of the overall complexity, but do not result in significant efficiency improvements.

V. COMPARATIVE EVALUATION OF MVAC-LVDC INTERFACES

Fig. 10 summarizes the efficiency and power density characteristics of the MVAC-LVDC conversion options discussed above. Today's MVAC-LVDC SSTs achieve demonstrated efficiencies of about 98% (modular industrial systems with LV SiC devices as well as academia prototypes employing upcoming 10 kV SiC devices). A combination of a modern highly efficient LFT and a high-performance LV SiC PFC rectifier can achieve at least the same efficiency and provides the same functionality as an SST (bidirectional power flow, reactive power processing, etc.), without the challenges of MV-connected power electronics or the need to control a massive amount of individual switches as in modular SST systems; proven LV high-power converter assembly and protection techniques are applicable, and the MV-side environment remains unchanged compared to today's systems. Accepting a reduced functionality (mostly unidirectional power flow, unregulated LVDC output voltage), highly robust 12-pulse rectifier systems that are complemented with active filters facilitate even more efficient power conversion thanks to the partial-power-processing approach. Both LFT-based solutions can furthermore easily be scaled to arbitrary MV levels without changing the requirements for the power electronics.

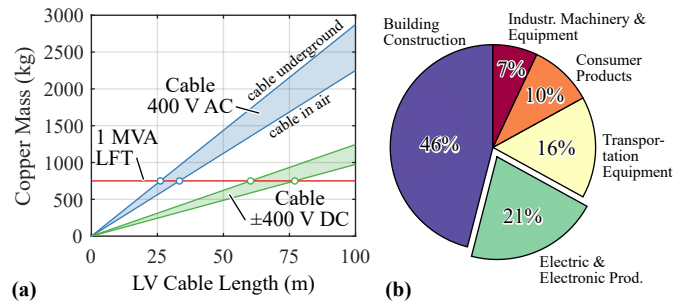


Fig. 11. (a) Comparison of the copper mass used in a 1 MVA LFT and in LV distribution cables for the same total power transfer at three-phase 400 V AC or ± 400 V DC, considering typical LV cables (Brugg Cables GKN 4). (b) Copper usage by sector in the U.S. (2021) [55].

Industrial SST prototypes do not achieve higher power densities than the discussed LFT-based solutions.¹² The gain in power density obtained from operating the isolation transformers at higher frequencies seems to be ultimately lost to the splitting of the power conversion into many small sub-units. This is highlighted by the fact that even when considering only the volume of the industrial SST prototype's (see **Section IV**) converter cells, the power density is in the order of that estimated for the LFT-based solutions. The overhead coming from assembly structures, isolation distances, and protection equipment such as the necessary MV-side filter chokes [43] further reduces the power density of the actual SST prototype.

Whereas it is true that LFTs clearly require more resources (mainly copper and silicon steel) than the smaller MFTs of SSTs, **Fig. 11a** highlights how the copper usage of the LV distribution wiring dwarfs that of an LFT; considering typical 400 V AC distribution cables, the amount of copper in an LFT suffices for covering a distance of less than 30 m. Similar considerations apply to busbars in datacenters (see **Fig. 2**). Note also that the electricity sector as a whole is far from dominating the overall copper demand (see **Fig. 11b**). Recycling of the metals in an LFT is relatively straightforward, in contrast to typical power electronic assemblies, which also feature much lower typical lifetimes (e.g., 10 yr vs. 40 yr for an LFT). A full comparison of the different MVAC-LVDC conversion options from a resource-usage or ecological standpoint would be important, but can thus not remain limited to looking at metal usage. Instead, it must include aspects such as embodied energy and recyclability, i.e., a life-cycle inventory (LCI) analysis [56]–[58] is needed, which is, however, beyond the scope of this paper.

Earlier studies have found that cost-wise, fully modular SSTs can't compete with LFTs in MVAC-LVAC applications, but less clear results have been obtained for MVAC-LVDC applications [40]. However, even a high-efficiency (Ecodesign) 1 MVA LFT can be bought for less than 15 kUSD [60]. Comparing a MMC-based SST (see **Fig. 9**) with a single MFT against an LFT-based solution, **Fig. 12** indicates that the LFT's cost must cover the entire SST's MV-side modular AC-

¹²Even a 3 MVA turn-key MV power station for interfacing a 1500 V DC PV system to a MV grid, which combines an LV inverter, an LFT, and all necessary switchgear in a standard 20 ft shipping container, achieves a higher $\rho \approx 0.08 \text{ kW/dm}^3$, although $\eta \approx 97.5\%$ remains lower (standard LFT with $\eta_{\text{LFT}} \approx 99\%$, silicon IGBTs instead of SiC MOSFETs resulting in a weighted CEC inverter efficiency of $\approx 98.5\%$) [54].

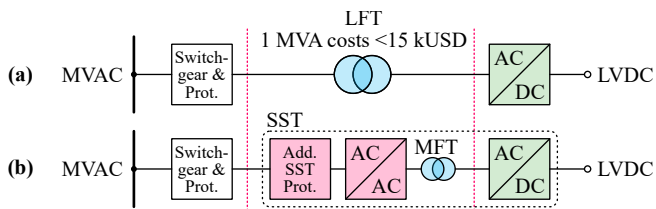


Fig. 12. Conceptual comparison of realization costs of MVAC-LVDC conversion with (a) an LFT and a SiC PFC rectifier or (b) an SST with a single MFT (such as shown in Fig. 9). The budget remaining for the SST’s MV-side protection, AC-AC power electronic conversion stage, and the MFT is thus less than 15 USD/kVA.

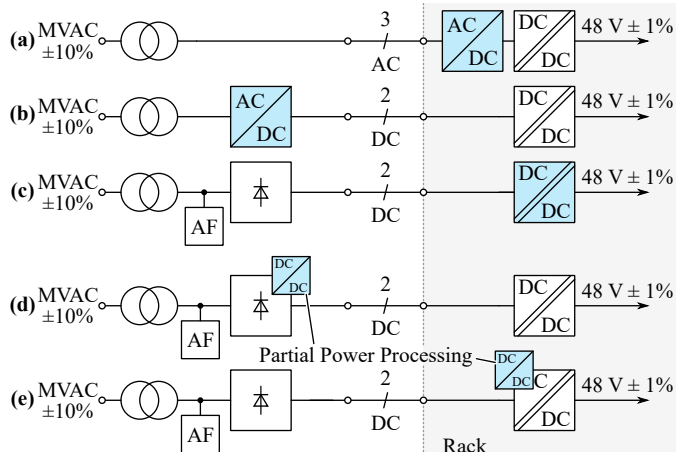


Fig. 13. Different locations of the stage that can compensate the grid voltage variations. (a) State-of-the-art rack-level or (b) centralized PFC rectifier. (c) 12-pulse rectifier with unregulated distribution voltage and rack-level DC-DC converters with regulation capability. Partial-power-processing regulating stages (d) in the rectifier or (e) in the DC-DC converters [59] for improved efficiency.

AC power electronics including potentially needed additional protection/overdimensioning (see, e.g., [43]) and the MFT, as the LV-side power electronics is similar in both cases (same voltage and power processed). As discussed above, the MFT may need less material than an LFT due to the higher operating frequency, but on the other hand more advanced manufacturing processes are needed (e.g., Litz wire windings, core materials with low high-frequency losses). Therefore, the budget for the SST’s MV-side power electronics is clearly <15 USD/kVA. Such low specific costs have been achieved for comparably simple automotive DC-AC drive inverters (10 USD/kW in 2017, 2.7 USD/kW R&D target for 2025) [61]. On the other hand, grid-connected PV inverters (again DC-AC inverters without isolation) show still significantly higher specific cost in the order of 30 USD/kW to 55 USD/kW [62]. Considering the additional effort needed for the MFT, MV-level isolation coordination and corresponding assembly structures, communication among the modules, cabinets, and specific protection equipment for relatively sensitive power electronics connected to the MV grid, cost-parity for MVAC-LVDC SSTs with LFT-based solutions seems not within easy reach.

Finally, in the context of datacenters, at least one stage in the conversion chain between the non-constant grid voltage and the ideally relatively constant 48 V DC voltage supplied to the IT equipment must provide the corresponding adaption capability, see Fig. 13. A central generation of a stable

±400 V DC distribution voltage would facilitate simplified rack-level 400 V/48 V DC-DC PSUs that could be realized as highly efficient unregulated DC transformers [63]. If, on the other hand, otherwise advantageous 12-pulse rectifiers are used, the rack-level DC-DC PSUs need to provide a certain voltage control range, which could be efficiently realized with partial-power-processing concepts such as [59].

VI. CONCLUSION

The presented analysis indicates that current industrial MVAC-LVDC SST demonstrators, for, e.g., datacenters or other applications such as high-power EV charging, do not outperform alternatives that retain the LFT and either complement it with LV-side high-efficiency SiC PFC rectifier systems (providing identical functionality) or employ robust 12-pulse rectifier systems with active filters (with reduced functionality, i.e., unidirectional power flow and no regulated LVDC voltage). SSTs face challenges regarding protection, robustness, and complexity, and are not easily scalable to arbitrary MV levels. Whether SST-based solutions can achieve cost-parity with LFT-based solutions even in the far future (volume production) is therefore in question.

Considering datacenter power supply architectures, we find that highest efficiency ($\eta_{\Sigma} \approx 98.2\%$, from MVAC to the input of the rack-level 400 V/48 V DC-DC PSUs) can be achieved with an 800 V DC (±400 V DC) distribution and a 12-pulse rectifier (with active filter) MVAC-LVDC interface. However, this has to be weighed against the system-level implications of a DC distribution system (e.g., impact on the protection concepts), especially in the light of similarly favorable efficiencies ($\eta_{\Sigma} \approx 97.8\%$) that can be achieved by means of an increase of the AC distribution voltage to 690 V. Ultimately, only full life-cycle-cost (LCC) analyses considering the entire power supply system can identify the overall best solution for a given application scenario.

REFERENCES

- [1] IEA, “Data centres and data transmission networks,” 2020. [Online]. Available: <https://tinyurl.com/2p8r4da8>
- [2] E. Masanet, A. Shehabi, N. Lei, S. Smith, and J. Koomey, “Recalibrating global data center energy-use estimates,” *Science*, vol. 367, no. 6481, pp. 984–986, Feb. 2020.
- [3] M. Koot and F. Wijnhoven, “Usage impact on data center electricity needs: A system dynamic forecasting model,” *Applied Energy*, vol. 291, p. 116798, Jun. 2021.
- [4] P. T. Krein, “Data center challenges and their power electronics,” *CPSS Trans. Power Electron. Appl.*, vol. 2, no. 1, pp. 39–46, 2017.
- [5] ABB Ltd., “EcoDry: The highest-efficiency dry-type transformers,” Apr. 2011. [Online]. Available: <https://tinyurl.com/2p52zv2n>
- [6] L. Schrittwieser, M. Leibl, M. Haider, F. Thöny, J. W. Kolar, and T. B. Soeiro, “99.3% efficient three-phase buck-type all-SiC SWISS rectifier for DC distribution systems,” *IEEE Trans. Power Electron.*, vol. 34, no. 1, pp. 126–140, Jan. 2019.
- [7] P. Sarti, “Facebook: Efficient power distribution: 277Vac distribution w/o centralized UPS, 95% high efficiency solution, battery cabinet as distributed backup energy unit,” in *2011 IEEE Hot Chips 23 Symp. (HCS)*, Stanford, CA, USA, Aug. 2011.
- [8] Delta Electronics, “Delta InfraSuite cast resin busway system brochure,” 2020. [Online]. Available: <https://tinyurl.com/56s7yhs6>
- [9] B. Hafez, H. S. Krishnamoorthy, P. Enjeti, S. Ahmed, and I. J. Pitel, “Medium voltage power distribution architecture with medium frequency isolation transformer for data centers,” in *Proc. 29th Annu. IEEE Appl. Power Electron. Conf. and Expo. (APEC)*, Fort Worth, TX, USA, Mar. 2014, pp. 3485–3489.
- [10] D. Rothmund, G. Ortiz, and J. W. Kolar, “SiC-based unidirectional solid-state transformer concepts for directly interfacing 400V DC to medium-voltage AC distribution systems,” in *Proc. 36th IEEE Int. Telecom. Energy Conf. (INTELEC)*, Vancouver, Canada, Sep. 2014.

- [11] S. Zhao, Q. Li, F. C. Lee, and B. Li, "High-frequency transformer design for modular power conversion from medium-voltage AC to 400 VDC," *IEEE Trans. Power Electron.*, vol. 33, no. 9, pp. 7545–7557, Sep. 2018.
- [12] D. Rothmund, T. Guillod, D. Bortis, and J. W. Kolar, "99% efficient 10 kV SiC-based 7 kV/400 V DC transformer for future data centers," *IEEE Trans. Emerg. Sel. Topics Power Electron.*, vol. 7, no. 2, pp. 753–767, Jun. 2019.
- [13] —, "99.1% efficient 10 kV SiC-based medium-voltage ZVS bidirectional single-phase PFC AC/DC stage," *IEEE Trans. Emerg. Sel. Topics Power Electron.*, vol. 7, no. 2, pp. 779–797, Jun. 2019.
- [14] Y. Kashihara, Y. Nemoto, W. Qichen, S. Fujita, R. Yamada, and Y. Okuma, "An isolated medium-voltage AC/DC power supply based on multi-cell converter topology," in *Proc. IEEE Appl. Power Electron. Conf. and Expo. (APEC)*, Tampa, FL, USA, Mar. 2017, pp. 2187–2192.
- [15] N. Soltan, H. Stage, R. W. De Doncker, and O. Apeldoorn, "Development and demonstration of a medium-voltage high-power DC-DC converter for DC distribution systems," in *Proc. 5th IEEE Int. Power Electron. for Distributed Generation Syst. Symp. (PEDG)*, Galway, Ireland, Jun. 2014.
- [16] M. Vasiladiotis, A. Rufer, and A. Beguin, "Modular converter architecture for medium voltage ultra fast EV charging stations: Global system considerations," in *Proc. IEEE Int. Electr. Vehicle Conf.*, Greenville, SC, USA, 2012.
- [17] H. Tu, H. Feng, S. Srdic, and S. Lukic, "Extreme fast charging of electric vehicles: A technology overview," *IEEE Trans. Transport. Electrific.*, vol. 5, no. 4, pp. 861–878, Dec. 2019.
- [18] C. Zhu, "High-efficiency, medium-voltage input, solid-state, transformer-based 400-kW/1000-V/400-A extreme fast charger for electric vehicles," Presented at the DOE Vehicle Techn. Off. Annu. Merit Rev. Electrification, Jun. 2019. [Online]. Available: <https://tinyurl.com/2vtyshxj>
- [19] —, "High-efficiency, medium-voltage input, solid-state, transformer-based 400-kW/1000-V/400-A extreme fast charger for electric vehicles," Presented at the DOE Vehicle Techn. Off. Annu. Merit Rev. Electrification, Jun. 2020. [Online]. Available: <https://tinyurl.com/2pcxn839>
- [20] —, "High-efficiency, medium-voltage input, solid-state, transformer-based 400-kW/1000-V/400-A extreme fast charger for electric vehicles," Presented at the DOE Vehicle Techn. Off. Annu. Merit Rev. Electrification, Jun. 2021. [Online]. Available: <https://tinyurl.com/4nnjbm7u>
- [21] X. Liang, S. Srdic, J. Won, E. Aponte, K. Booth, and S. Lukic, "A 12.47 kV medium voltage input 350 kW EV fast charger using 10 kV SiC MOSFET," in *Proc. IEEE Appl. Power Electron. Conf. and Expo. (APEC)*, Anaheim, CA, USA, Mar. 2019, pp. 581–587.
- [22] J. Solanki, N. Fröhleke, J. Böcker, A. Averberg, and P. Wallmeier, "High-current variable-voltage rectifiers: State of the art topologies," *IET Power Electron.*, vol. 8, no. 6, pp. 1068–1080, 2015.
- [23] R. Unruh, F. Schafmeister, N. Fröhleke, and J. Böcker, "1-MW full-bridge MMC for high-current low-voltage (100V–400V) DC-applications," in *Proc. Power Electron. and Intelligent Motion Conf. (PCIM Europe)*, Nuremberg, Germany, Jul. 2020.
- [24] J. E. Huber and J. W. Kolar, "Volume/weight/cost comparison of a 1 MVA 10 kV/400 V solid-state against a conventional low-frequency distribution transformer," in *Proc. IEEE Energy Conv. Congr. and Expo. (ECCE USA)*, Pittsburgh, PA, USA, Sep. 2014, pp. 4545–4552.
- [25] Schneider Electric, "Altivar AFE VV3A7258 datasheet," 2021.
- [26] M. Meyer, *Leistungselektronik – Einführung. Grundlagen. Überblick (in German)*. Berlin Heidelberg: Springer-Verlag, 1990.
- [27] J. K. Hall, J. G. Kettleborough, and A. B. M. J. Razak, "Parallel operation of bridge rectifiers without an interbridge reactor," *IEE Proc. B (El. Power. Appl.)*, vol. 137, no. 2, pp. 125–140, Mar. 1990.
- [28] Y.-S. Tzeng, N. Chen, and R.-N. Wu, "Modes of operation in parallel-connected 12-pulse uncontrolled bridge rectifiers without an interphase transformer," *IEEE Trans. Ind. Electron.*, vol. 44, no. 3, pp. 344–355, Jun. 1997.
- [29] Y.-S. Tzeng, "Harmonic analysis of parallel-connected 12-pulse uncontrolled rectifier without an interphase transformer," *IEE Proc. B (El. Power. Appl.)*, vol. 145, no. 3, pp. 253–260, May 1998.
- [30] C.-C. Hou and C.-H. Tsai, "Design of an auxiliary converter for 12-pulse diode rectifiers," in *Proc. 3rd IEEE Int. Future Energy Electron. Conf. (IFEE/ECCE Asia)*, Kaohsiung, Taiwan, Jun. 2017, pp. 231–235.
- [31] S. Bala, D. Das, E. Aeloiza, A. Maitra, and S. Rajagopalan, "Hybrid distribution transformer: Concept development and field demonstration," in *Proc. IEEE Energy Conv. Congr. and Expo. (ECCE USA)*, Raleigh, NC, USA, Sep. 2012, pp. 4061–4068.
- [32] J. Burkard and J. Biela, "Evaluation of topologies and optimal design of a hybrid distribution transformer," in *Proc. 17th Europ. Power Electron. and Appl. Conf. (EPE)*, Geneva, Switzerland, Sep. 2015.
- [33] J. W. Kolar, T. B. Soeiro, J. Biela, P. Ranstad, and J. Linner, "Method to minimize input current harmonics of power systems such as ESP power systems," US Patent 9,331,561 B2, May, 2016.
- [34] T. Soeiro, J. Biela, J. Linner, P. Ranstad, and J. W. Kolar, "Line power quality improvement for ESP systems using multi-pulse and active filter concepts," in *Proc. 36th Annu. IEEE Ind. Electron. Soc. Conf. (IECON)*, Glendale, AZ, USA, Nov. 2010, pp. 538–543.
- [35] J. W. Kolar, F. Krismer, Y. Lobsiger, J. Mühlethaler, T. Nussbaumer, and J. Miniböck, "Extreme efficiency power electronics," in *Proc. 7th Int. Integrated Power Electron. Syst. Conf. (CIPS)*, Nuremberg, Germany, Mar. 2012.
- [36] H. Ertl, J. W. Kolar, and F. C. Zach, "A constant output current three-phase diode bridge employing a novel 'electronic smoothing inductor,'" in *Proc. Power Electron. and Intelligent Motion Conf. (PCIM Europe)*, Nuremberg, Germany, 1999.
- [37] N. Raju, A. Daneshpooy, and J. Schwartzberg, "Harmonic cancellation for a twelve-pulse rectifier using DC bus modulation," in *Conf. Rec. 37th IEEE Ind. Appl. Soc. (IAS) Annu. Meet.*, Pittsburgh, PA, USA, Oct. 2002, pp. 2526–2529.
- [38] U. Drogenik, G. Laimer, and J. W. Kolar, "Theoretical converter power density limits for forced convection cooling," in *Proc. Power Electron. and Intelligent Motion Conf. (PCIM Europe)*, no. 4, Nuremberg, Germany, Jun. 2005, pp. 608–619.
- [39] J. Solanki, N. Fröhleke, and J. Böcker, "Implementation of hybrid filter for 12-pulse thyristor rectifier supplying high-current variable-voltage DC load," *IEEE Trans. Ind. Electron.*, vol. 62, no. 8, pp. 4691–4701, Aug. 2015.
- [40] J. E. Huber and J. W. Kolar, "Applicability of solid-state transformers in today's and future distribution grids," *IEEE Trans. Smart Grid*, vol. 10, no. 1, pp. 317–326, Jan. 2019.
- [41] C. Zhao, D. Dujic, A. Mester, J. K. Steinke, M. Weiss, S. Lewdeni-Schmid, T. Chaudhuri, and P. Stefanutti, "Power electronic traction transformer—Medium voltage prototype," *IEEE Trans. Ind. Electron.*, vol. 61, no. 7, pp. 3257–3268, Jul. 2014.
- [42] W. van der Merwe and T. Mouton, "Solid-state transformer topology selection," in *Proc. IEEE Int. Ind. Techn. Conf. (ICIT)*, Gippsland, VIC, Australia, Feb. 2009.
- [43] T. Guillod, F. Krismer, and J. W. Kolar, "Protection of MV converters in the grid: The case of MV/LV solid-state transformers," *IEEE Trans. Emerg. Sel. Topics Power Electron.*, vol. 5, no. 1, pp. 393–408, Mar. 2017.
- [44] B. Engel, M. Victor, G. Bachmann, and A. Falk, "15 kV/16.7 Hz energy supply system with medium frequency transformer and 6.5 kV IGBTs in resonant operation," in *Proc. 10th Europ. Power Electron. and Appl. Conf. (EPE)*, Toulouse, Frankreich, Sep. 2003.
- [45] H. S. Krishnamoorthy, P. Garg, and P. N. Enjeti, "A new medium-voltage energy storage converter topology with medium-frequency transformer isolation," in *Proc. IEEE Energy Conversion Congr. and Expo. (ECCE USA)*, Raleigh, NC, USA, Sep. 2012, pp. 3471–3478.
- [46] L. T. Keister, J. D. Keister, B. J. Schafer, and A. A. M. Esser, "Power management utilizing a high-frequency low voltage pre-charge and synchronous common coupling," US Patent 9906155B2, Feb., 2018.
- [47] T. Chaudhuri, M. A. Faedy, and S. Isler, "Gewichtige Vorteile (in German)," *ABB Review*, no. 4, pp. 25–29, 2016.
- [48] J. W. Kolar and J. E. Huber, "Fundamentals and application-oriented evaluation of solid-state transformer concepts," in *Tutorial presented at the Southern Power Electron. Conf. (SPEC)*, Auckland, New Zealand, Dec. 2016.
- [49] Resilient Power, "Containerized supercharging station," 2021. [Online]. Available: <https://www.resilientpower.com/>
- [50] W. McMurray, "Fast response stepped-wave switching power converter circuit," U.S. Patent 3,581,212, May, 1971.
- [51] A. Alesina and M. Venturini, "Solid-state power conversion: A Fourier analysis approach to generalized transformer synthesis," *IEEE Trans. Circuits. Syst.*, vol. 28, no. 4, pp. 319–330, Apr. 1981.
- [52] M. Glinka and R. Marquardt, "A new AC/AC multilevel converter family," *IEEE Trans. Ind. Electron.*, vol. 52, no. 3, pp. 662–669, Jun. 2005.
- [53] Y. P. Marca, M. G. Roes, J. L. Duarte, and K. G. Wijnands, "Isolated MMC-based ac/ac stage for ultrafast chargers," in *Proc. 30th Int. IEEE Ind. Electron. Symp. (ISIE)*, Kyoto, Japan, Jun. 2021.
- [54] SMA Solar Technology, "MV Power Station 2200 / 2475 / 2500 / 2750 / 3000," 2018. [Online]. Available: <https://tinyurl.com/yckpfsnz>
- [55] D. M. Flanagan, "Mineral commodity summaries: Copper," 2022. [Online]. Available: <https://tinyurl.com/mrx6t94p>
- [56] J. Popović-Gerber, J. A. Ferreira, and J. D. van Wyk, "Quantifying the value of power electronics in sustainable electrical energy systems," *IEEE Trans. Power Electron.*, vol. 26, no. 12, pp. 3534–3544, Dec. 2011.
- [57] A. Nordelöf, M. Alatalo, and M. L. Söderman, "A scalable life cycle inventory of an automotive power electronic inverter unit—Part I: Design and composition," *Int. J. Life Cycle Assess.*, vol. 24, no. 1, pp. 78–92, Jan. 2019.
- [58] A. Nordelöf, "A scalable life cycle inventory of an automotive power electronic inverter unit—Part II: Manufacturing processes," *Int. J. Life Cycle Assess.*, vol. 24, no. 4, pp. 694–711, Apr. 2019.
- [59] D. Neumayr, M. Vöhringer, N. Chrysogelos, G. Deboy, and J. W. Kolar, "P3DCT—Partial-power pre-regulated DC transformer," *IEEE Trans. Power Electron.*, vol. 34, no. 7, pp. 6036–6047, Jul. 2019.
- [60] Tesar S.r.l., "Ecodesign Transformers," 2020. [Online]. Available: <https://tinyurl.com/bdfbj47>
- [61] U.S. Drive, "Electrical and electronics technical team roadmap," Oct. 2017. [Online]. Available: <https://tinyurl.com/5akv6rs4>
- [62] Fraunhofer Institute for Solar Energy Systems (ISE), "Photovoltaics Report," Feb. 2022. [Online]. Available: <https://tinyurl.com/4649dy33>
- [63] J. E. Huber, J. Miniböck, and J. W. Kolar, "Generic derivation of dynamic model for half-cycle DCM series resonant converters," *IEEE Trans. Power Electron.*, vol. 33, no. 1, pp. 4–7, Jan. 2018.